TIME-LAPSE SEISMIC INTERPRETATION IN τ-p SPACE USING PRE-STACK DATA

YAN-XIAO HE[1], DOUG A. ANGUS[1], SAN-YI YUAN[2], THOMAS D. BLANCHARD[3], ROGER A. CLARK[1] and MARK W. HILDYARD[1]

[1] *School of Earth and Environment, University of Leeds, Leeds, LS2 9JT, U.K.*
[2] *Department of Geophysics and Information Engineering, China University of Petroleum, Beijing, P.R. China.*
[3] *Total E&P UK Ltd., Geoscience Research Centre, Aberdeen, U.K.*
eeyhe123@gmail.com

(Received March 4, 2015; revised version accepted September 13, 2015)

ABSTRACT

He, Y.-X., Angus, D.A., Yuan, S.-Y., Blanchard, T.D., Clark, R.A. and Hildyard, M.W., 2015. Time-lapse seismic interpretation in τ-p space using pre-stack data. *Journal of Seismic Exploration*, 24: 475-496.

We present a new algorithm to measure time-lapse vertical traveltime shifts in seismic pre-stack shot and CMP gathers by tracking traces having constant horizontal slowness in τ-p space. Unlike other methods for measuring these attributes from stacked volumes, our use of pre-stack data avoids errors and uncertainties inevitably introduced in conventional time-lapse processing, such as choosing a suitable migration velocity model and cross-correlation time-window size. Results are localised to a given interval and thus free from overburden effects. This approach is used to estimate layer vertical traveltime shifts, a reservoir compaction-dilation coefficient, and hence calculate both velocity and thickness changes within a reservoir and the overburden. We demonstrate the method using synthetic reflection data generated using both a ray-based and a finite-difference full-waveform algorithms on two suites of models: a simple four-layer reservoir model; and a hydro-mechanical simulation model. We compare our estimates of layer interval vertical time-lapse traveltime shifts and velocity and thickness changes with those of the input model. The results indicate that the new τ-p time-lapse method produces sufficiently accurate results compared to conventional methods.

KEY WORDS: time-lapse seismic, τ-p domain, hydro-mechanical model, rock physics.

0963-0651/15/$5.00

INTRODUCTION

The technique of time-lapse seismic reservoir monitoring provides a useful tool in evaluating these subsurface physical changes using repeated seismic surveys, where changes in seismic travel-time and reflection amplitude are linked with rock physics modelling to provide an estimate of velocity change and strain. To optimize reservoir characterization and production strategies, it is important to distinguish between fluid saturation and geomechanical effects, which requires the ability to differentiate between velocity and layer thickness changes using time-lapse seismic data. Conventional time-lapse seismic processing often involves post-stack data analysis and migration, and requires assumptions about the changes occurring in the subsurface that may or may not be appropriate. As such, there is potential for uncertainty in post-stack time-lapse seismic interpretation, for instance migration velocity model in "parallel processing" (e.g., He et al., 2015a). The traveltime difference is one of the key time-lapse seismic attributes used to estimate subsurface layer thickness and velocity changes. However, unless changes in the reservoir are laterally homogeneous at least on the scale of the seismic gather, special care might be required within time-lapse seismic processing to handle induced lateral velocity heterogeneity (e.g., Cox and Hatchell, 2008; He et al., 2015b, in review).

Recently, there has been interest in using pre-stack seismic data in time-lapse seismic analysis and this is because geomechanical effects (e.g., Angus et al., 2011) could introduce complications in conventional time-lapse processing workflows. From a modelling perspective, Fuck et al. (2009) derive an analytic expression to measure three-dimensional stress-related traveltime shifts due to velocity changes and rock deformation within the pre-stack domain. Smith and Tsvankin (2012) integrate geomechanical and seismic full-waveform simulation to investigate the influence of reservoir compaction-induced changes using measured traveltime shifts from reflected and converted P-, S- and PS-waves from pre-stack shot-gather data. From an observational perspective, Røste et al. (2006) measure time-lapse traveltime shifts by interpolating the seismic series first within a time window and picking for the maximum amplitude peak for pre-stack gather, and hence detect traveltime shifts of 1 ms. Ghaderi and Landrø (2009) introduce a method to calculate changes in thickness and velocity within individual layers using a combination of traveltime shift and amplitude change estimates from time-lapse seismic pre-stack data.

In this paper, a new algorithm for estimating the time-lapse seismic vertical traveltime shifts for laterally heterogeneous and anisotropic layers using the τ-p transform and pre-stack gathers is introduced (He and Angus, 2014). The time-lapse τ-p transform method provides a process to estimate vertical traveltime for individual layers using pre-stack gathers, and hence extract time-lapse vertical traveltime shifts, which are compared with the measurements using a conventional cross-correlation method and post-stack migrated data. The new pre-stack gather τ-p transform traveltime shift estimation method seeks to improve the effectiveness of the measured time-lapse attributes with respect to post-stack methods by reducing the uncertainty due to the stress-induced velocity changes that can be laterally heterogeneous and anisotropic. We apply a 1D (vertical strain) rock physics model [parameterised through the so-called R-factor (Hatchell and Bourne, 2005), or the equivalent α-factor (Røste et al., 2005)] to link seismic velocity and vertical strain changes. In this approach the strain coefficient or α-factor is estimated from zero-offset as well as offset-dependent traveltime shifts for individual layers (see Røste et al., 2006). The method is tested on a suite of two subsurface elastic reservoir models: a simple four-layer reservoir model, and a complex deep reservoir model undergoing depletion based on output from numerical hydro-mechanical simulation. The estimated vertical traveltime shifts, vertical velocity and layer thickness changes from the models are compared with the respective true subsurface elastic model values.

METHODOLOGY

In this section, the new τ-p domain pre-stack layer interval vertical traveltime shift estimation (τ-p PSITS) method is introduced. We first review the expressions for reflection traveltime and the τ-p transform for a horizontal, homogeneous layered medium. We then introduce the formulations to compute vertical traveltime for individual layers for both the isotropic and anisotropic cases. Next, a workflow is introduced to calculate the time-lapse seismic traveltime shifts and subsequently discriminate between time-lapse changes in vertical velocity and layer thickness for individual layers. The discrimination approach is based on the method proposed by Røste et al. (2006) using the 1D rock-physics α-factor.

The τ-p transform

The advantage of interpreting seismic reflection data using the τ-p transform (e.g., Chapman, 1981) has been highlighted in several studies (e.g., van der Baan and Kendall, 2002 and 2003; Reine et al., 2012). Utilizing matched events for a constant horizontal slowness, the traveltime within an i-th layer (τ_i) can be computed by subtracting the overburden traveltime from the total intercept time (τ) (e.g., Kappus et al., 1990). This can be done because overlapping events in the t-x space are separated in the τ-p domain. Based on these principles, the interval two-way traveltime and the vertical traveltime can be calculated for individual layers using seismic pre-stack gather data (i.e., shot gathers and common midpoint gathers). In the τ-p domain, the reflection traveltime expression can be described as the sum of vertical and horizontal slowness components. Diebold et al. (1981) and Stoffa et al. (1981) introduce a velocity-depth inversion method and show that the vertical component of traveltime is the cumulative product of vertical slowness and layer thickness. van der Baan and Kendall (2002, 2003) utilize the τ-p transform method to compute move-out curves for primary reflected and converted waves for laterally homogeneous, layered transversely isotropic (VTI) and horizontal transverse isotropic (HTI) media. They show that the differential intercept time for each layer can be calculated by applying the so-called bottom-up layer-stripping scheme. Reine et al. (2012) map t-x space pre-stack common midpoint (CMP) data to the τ-p domain to measure the layer interval attenuation for each single layer by tracking each trace having constant horizontal slowness.

For horizontal and laterally homogeneous layers, the same reflection traveltime expression applies for both common-shot and CMP geometries since horizontal slowness is conserved (i.e., constant along the ray path). In the presence of dipping layers, horizontal slowness is not constant along the ray path. For dipping layers, however, Diebold and Stoffa (1981) show that the effective horizontal slowness is the average of the up-coming and the down-going ray horizontal slowness for pre-stack CMP gathers.

The traveltime versus offset equation for a reflection from a horizontal layer at depth z in an isotropic homogeneous medium can be described as sum of the vertical and horizontal components of slowness along the ray path in 2D (e.g., van der Baan and Kendall, 2002)

$$t = (\partial t/\partial x)x + 2(\partial t/\partial z)z = px + 2qz \quad , \tag{1}$$

where t is the two-way traveltime, x is the source-receiver offset, p and q are the horizontal and vertical slowness respectively. From the stacking velocity v $= (p^2 + q^2)^{(-1/2)}$, the horizontal slowness can be expressed as p $= \sin\theta/v$ and the vertical slowness expressed as q $= \cos\theta/v$, where θ is the incidence angle. Using a zero-offset intercept time (i.e., τ) and the instantaneous slope (i.e., p), the reflection traveltime curve in the t-x domain can be directly transformed to the slowness domain (e.g., Diebold and Stoffa, 1981; Kappus et al., 1990)

$$t = \tau + px \quad . \tag{2}$$

Thus, the total intercept time can then be expressed as

$$\tau = 2\sum_{i=1}^{N} q_i z_i = t - px \quad , \tag{3}$$

where z_i is the vertical thickness in the i-th layer. Eq. (3) can be used to isolate contributions of individual layers on reflection traveltime via employing the so-called bottom-up layer-stripping method (e.g., van der Baan and Kendall, 2002).

For pure body-wave modes travelling in transversely isotropic (TI) media consisting of flat homogeneous and horizontal layers, van der Baan and Kendall (2002, 2003) describe the anisotropic reflection move-out τ_i as

$$\tau_i^2/\tau_{0,i}^2 = (2z_iq_i)^2/(2z_i/v_{0,i})^2 = (v_{0,i}^2/v_{ph,i}^2)(1 - p^2v_{ph,i}^2) \quad , \tag{4}$$

where $q_i^2 = v_{ph,i}^{-2} - p^2$, $v_{ph,i}$ is the phase velocity in the i-th layer, $v_{0,i}$ is the phase velocity for a vertically traveling wave, and $\tau_{0,i}$ is the two-way interval traveltime for normal-incidence propagation. Within the i-th layer, the anisotropic move-out τ_i can be expressed in the τ-p domain

$$\tau_i = \tau_{0,i}v_{0,i}\sqrt{\{(1/v_{ph,i}^2) - p^2\}} \quad . \tag{5}$$

Thus the zero-offset traveltime for interval intercept $\tau_{0,i}$ can be expressed as

$$\tau_{0,i} = \tau_i/v_{0,i}\sqrt{\{(1/v_{ph,i}^2) - p^2\}} \quad . \tag{6}$$

For the isotropic case, eq. (4) reduces to $\tau_i^2 = \tau_{0,i}^2(1 - p^2v_{0,i}^2)$.

Using the approximation of Alkhalifah (1998), van der Baan and Kendall (2002, 2003) derive a two-parameter approximation of the τ_i(p) curves for P-wave reflections

$$\tau_i = \tau_{0,i}[1 - p^2v_i^2/(1 - 2\eta_ip^2v_i^2)]^{1/2} \quad , \tag{7}$$

which can be used to track individual reflections for a defined interface. Thus the zero-offset travel-time in each isolated layer can be correctly recovered using the expression

$$\tau_{0,i} = \tau_i[1 - p^2v_i^2/(1 - 2\eta_ip^2v_i^2)]^{-1/2} \quad , \tag{8}$$

where $v_i = \alpha_0\sqrt{(1 + 2\delta)}$ is the P-wave interval stacking velocity, $\eta = (\varepsilon - \delta)/(1 + 2\delta)$ is the anisotropy parameter assuming weak anisotropy (Alkhalifah and Tsvankin, 1995), and ε and δ are the Thomsen (1986) parameters. The symbol α_0 is the vertical P-wave velocity. For the isotropic case (i.e., $\eta = 0$), the τ_i(p) move-out curve in each layer reduces to

$$\tau_i = \tau_{0,i}(1 - p^2v_i^2)^{1/2} \quad , \tag{9}$$

and hence the traveltime for normal incidence is rewritten as

$$\tau_{0,i} = \tau_i(1 - p^2v_i^2)^{-1/2} \quad . \tag{10}$$

Thus for time-lapse pre-stack seismic P-wave subcritical reflection data, time-lapse seismic traveltime shifts of zero-offset within a chosen layer can be measured in the τ-p domain using eq. (8) for the anisotropic case and eq. (10) for the isotropic case

$$\Delta T_{0,i} = \tau_{0,i}(\text{monitor}) - \tau_{0,i}(\text{baseline}) \quad . \tag{11}$$

Discrimination velocity and thickness changes using a compaction-dilation coefficient

Since time-lapse traveltime shifts capture the combined contributions of velocity and thickness changes within a layer, the vertical relative time-lapse traveltime shifts can be represented (e.g., Landrø and Stammeijer, 2004) by assuming small velocity and layer thickness changes

$$\Delta T_0/T_0 \approx (\Delta z/z) - (\Delta v/v) \quad , \tag{12}$$

where T_0 is the vertical layer interval traveltime, and Δ represents the change in the respective parameters between the baseline and monitor surveys. Subsequently, Hatchell and Bourne (2005) and Røste et al. (2005) introduce an equivalent 1D velocity-strain coupling coefficient model to link velocity changes ($\Delta v/v$) and vertical strain changes ($\varepsilon_{zz} = \Delta z/z$). The models employ the relative traveltime shifts of normal-incidence [eq. (12)] to discriminate reservoir compaction-induced changes for both vertical velocity and thickness for a reservoir and the overburden layers.

For the case when vertical strain is non-negligible, the vertical traveltime shift is the sum of vertical velocity change and strain. Assuming $\Delta z/z \ll 1$, eq. (12) can be rewritten as

$$\Delta T_0/T_0 \approx [\Delta z/(z+\Delta z)] - [\Delta v/(v+\Delta v)] \quad . \tag{13}$$

The 1D rock physics models of Hatchell and Bourne (2005) and Røste et al. (2005) are based on eq. (13) and introduce a dimensionless coefficient (e.g., the R-factor or α-value) to link the relative velocity change and vertical strain

$$[\Delta v/(v+\Delta v)] = -R\cdot[\Delta z/(z+\Delta z)] \quad . \tag{14}$$

Combining eqs. (13) with (14), the changes in vertical velocity and strain can be calculated as

$$\Delta v = -(\Delta T_0/T_0)\cdot R\cdot v\cdot[1 + R(\Delta T_0/T_0)]^{-1} \quad , \tag{15}$$

and

$$\Delta z = (\Delta T_0/T_0)\cdot z\cdot[1 + R - (\Delta T_0/T_0)]^{-1} \quad . \tag{16}$$

Utilizing zero-offset and offset-dependent traveltime shifts for time-lapse seismic pre-stack data, Røste et al. (2006) estimate the dimensionless α-value by solving the following equation

$$\Delta T(x_0,d)/T(x_0,d) = \{z^2(x_0)/[z^2(x_0)+d^2]\}[1/(1-\alpha)][\Delta T_0(x_0)/T_0(x_0)] - (1/2h)[\alpha/(1-\alpha)] \int_{x_0-d}^{x_0+d} dx[\Delta T_0(x)/T_0(x)] \quad , \tag{17}$$

using a least-square approach. Here, x_0 is the reference point (i.e., CMP position), d is the half source-receiver offset, and the relative change in vertical two-way traveltime at position x_0 is $\Delta T_0(x_0)/T_0(x_0)$. The relative change in two-way traveltime (left-hand part) at position x_0 for half-offset d is $\Delta T(x_0,d)/T(x_0,d)$, which is computed from pre-stack data using acquisition geometry relationship and the vertical traveltime $\tau_{0,i}$ for each individual layer. The compaction-dilation factor α is then determined using least-square and minimization of the relative changes in two-way traveltime $\Delta T(x_0,d)/T(x_0,d)$ between the predicted [in eq. (17)] and the true model values. Thus the layer interval vertical velocity change Δv and thickness change Δz can be calculated from eqs. (15) and (16) using the relative change in vertical traveltime $\Delta T_0(x_0)/T_0(x_0)$ and the α-value.

Our proposed τ-p PSITS workflow can be summarised as follows. First, seismic pre-stack data (shot gather or CMP gather) are transformed to the τ-p domain [eq. (2)]. Next, τ(p) curves are tracked for chosen reflection events where the bottom-top layer stripping strategy is implemented to compute the differential intercept time $\Delta\tau_i = \tau_i - \tau_{i-1}$ for each horizontal slowness for individual layers. The vertical two-way traveltime $\tau_{0,i}$ is calculated for the i-th layer for either the anisotropic case using eq. (8) or for the isotropic case using eq. (10). And subsequently, the method of Røste et al. (2006) is applied to estimate the 1D α-value utilizing the calculated zero-offset and offset-dependent traveltime shifts [eq. (17)]. Finally, changes in vertical velocity and layer thickness are computed for individual layers using eqs. (15) and (16).

NUMERICAL EXAMPLES

In this section, several numerical tests are presented to demonstrate the applicability of the τ-p transform pre-stack time-lapse seismic analysis method. The first suite of models are based on a simple four-layer reservoir geometry. In these models we examine the influence of velocity and layer thickness changes, dipping layers, and induced anisotropy on measured vertical traveltime shifts between the baseline and monitor surveys (e.g., see Fig. 1a). The second model is a complex deep reservoir model undergoing compaction due to effective stress changes within the reservoir, leading to strain and velocity change in the over-burden (He et al., 2015b). The model is used to evaluate how well the τ-p transform method to estimate interval vertical travel-time shifts for a more complicated geometry. Specifically, the model is applied to demonstrate the effectiveness of τ-p transform time-lapse analysis method for more realistic synthetics for underground models having non-planar surfaces and heterogeneous velocity distribution.

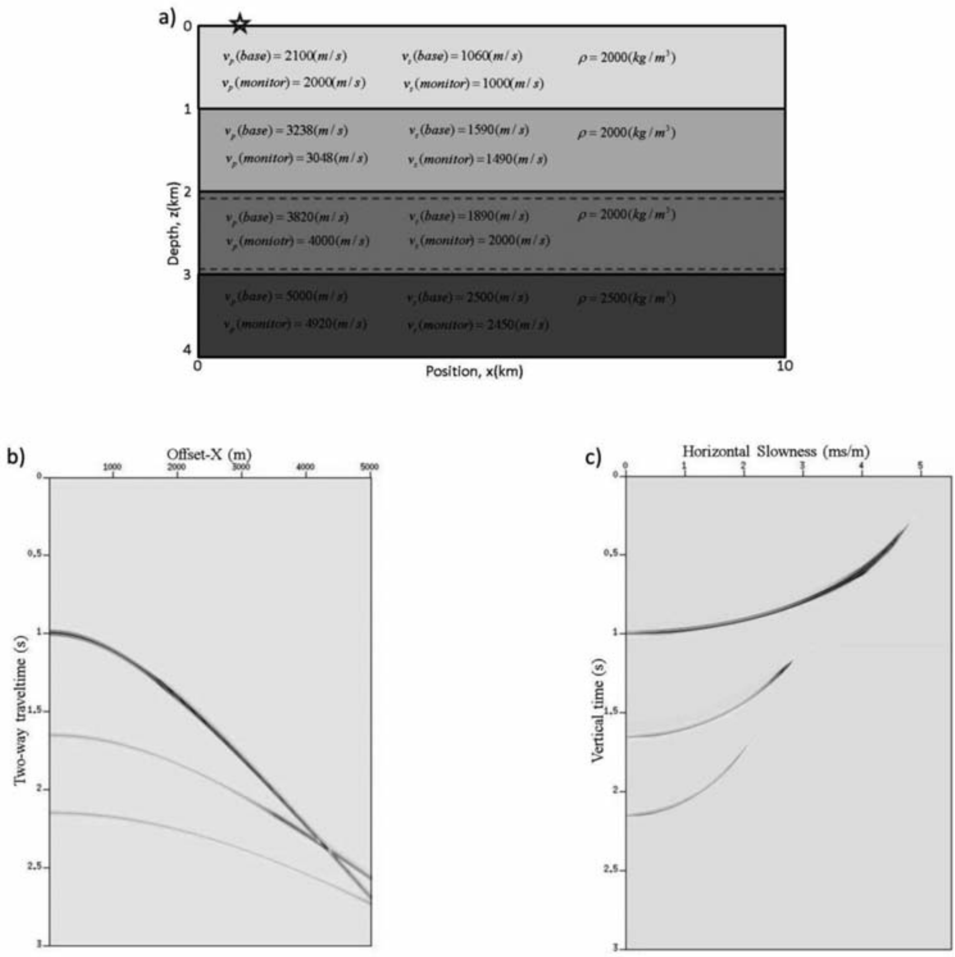

Fig. 1. Schematic diagram of the synthetic four-layer reservoir baseline and monitor models (a) utilized to generate synthetic ray-based waveform shot gathers in the t-x domain (b) and mapped to the τ-p domain (c). The grey-dashed lines in (a) represent the change in the reservoir interfaces (top and bottom) in monitor model.

Using these elastic models, we generate synthetic 2D reflection seismic data-sets using the anisotropic ray tracer ATRAK (Guest and Kendall, 1993) and the isotropic finite-difference (FD) full-waveform simulator E3D (Larsen et al., 2001). The anisotropic ray tracer allows efficient computation of synthetic waveforms in smoothly varying generally anisotropic models, with the particular advantage of modelling only primary reflections and avoiding complications due to multiples (see Fig. 1b). The source is a zero-phase Ricker wavelet with the central frequency of 30 Hz and time sample of 1 ms. We use a receiver spacing of 12.5 m, with a minimum offset of 200 m and a maximum offset of 5000 m. Thus the time and spatial sampling are sufficient to guarantee the absence of artefacts (e.g., alias and truncation) in the synthetic datasets. Also we generate the FD full-waveform synthetics to simulate more realistic seismograms via including the influence of multiples within the τ-p workflow to assess the magnitude of error due to non-primary signal noise. Since the acquisition geometry and wavelet frequency are constant for all simulations (baseline and monitor surveys), there are no issues related to time-lapse repeatability.

Horizontal four-layer reservoir model

Fig. 1(a) shows the horizontal four-layer reservoir model, where the reservoir unit is the third layer. The two red-dashed lines indicate the layer thickness change for the monitor model between the top and bottom reservoir interfaces. This scenario depicts homogeneous reservoir depletion with homogeneous rock compaction and velocity change throughout the reservoir and surrounding rocks. Three hyperbolic traveltime curves for P-P wave reflections from three horizons (see Fig. 1b) are mapped onto the elliptic move-out curves in the τ-p domain (see Fig. 1c). The vertical traveltimes for the baseline and monitor models for the three horizons (i.e., overburden, top reservoir and bottom reservoir) are computed using eq. (10) by tracking the τ_i(p) curves, where the Hilbert transform is implemented to narrow the bandwidth and magnify the amplitude. The time-lapse vertical travel-times are used to calculate time-lapse traveltime shifts in each individual layer [eq. (11)].

Fig. 2(a) shows the vertical traveltime shifts measured using the seismic pre-stack gather and τ-p transform method for the three interfaces. Fig. 2(b) shows the error in the traveltime shifts estimates and represents the difference between the estimated and true reservoir model values. For all three horizons, the errors are within less than ± 1.5 ms for the entire offset range which is below the typical noise level (see Landrø and Stammeijer, 2004). This indicates that the time-lapse τ-p transform method can provide accurate estimates of individual layer traveltime shifts using pre-stack gathers. For homogeneous, isotropic and horizontal layers, the τ-p approach can be more accurate than conventional methods for measuring time-lapse traveltime shifts, such as maximum cross-correlation method using post-stack seismic data (e.g., He et al., 2015a). Nevertheless, it should be noted that application of the τ-p transform, modifying the signal bandwidth using a Hilbert transform and tracking τ_i(p) curves might introduce artificial noise (i.e., errors) in the final time-shift estimates. This can be seen in Fig. 2(b) as fluctuations in the error curves. However, these errors are small (less than ± 1 ms, or $\pm 3\%$) and so are insignificant compared to other sources of error in real data.

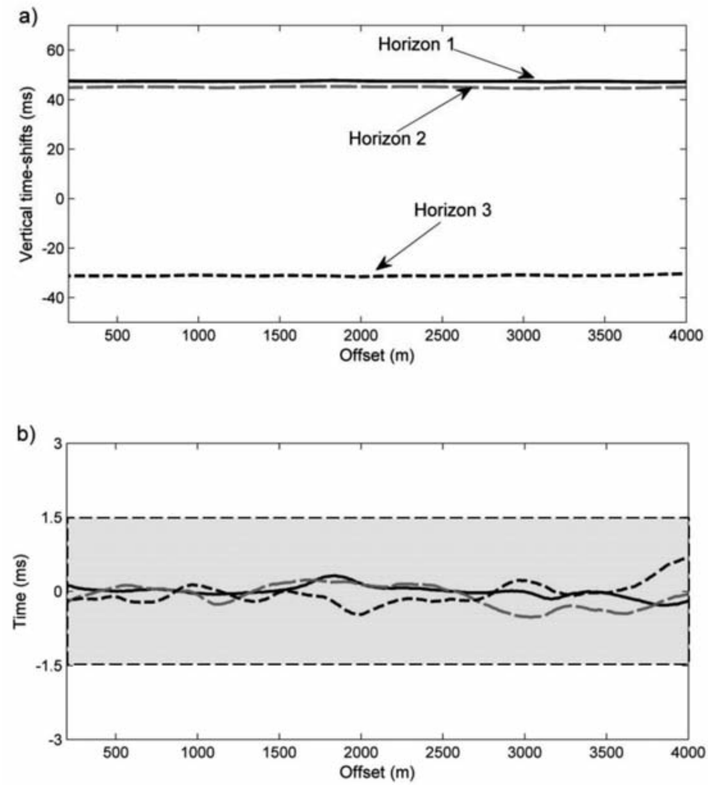

Fig. 2. The time-lapse seismic vertical traveltime shifts (a) for three horizons (i.e., overburden, top reservoir and bottom reservoir), and the errors (b) in the estimates calculated with respect to the true reservoir model values. In this figure, the black solid curve represents the overburden horizon, the grey long dashed curve represents the top reservoir horizon, and the black short dashed curve represents the bottom reservoir horizon. In (b), the grey box indicates the maximum tolerable error of ± 1.5 ms.

Fig. 3 displays the calculated changes in vertical velocity and layer thickness for the three horizons. The velocity and layer thickness changes are estimated from the vertical traveltime shifts using the true R-value of the reservoir layer using eqs. (14), (15) and (16). The estimates are in good agreement with the true model values, with maximum errors of ± 5 m/s (or $\pm 2.6\%$) for velocity change and ± 1 m (or $\pm 6.7\%$) for layer thickness change.

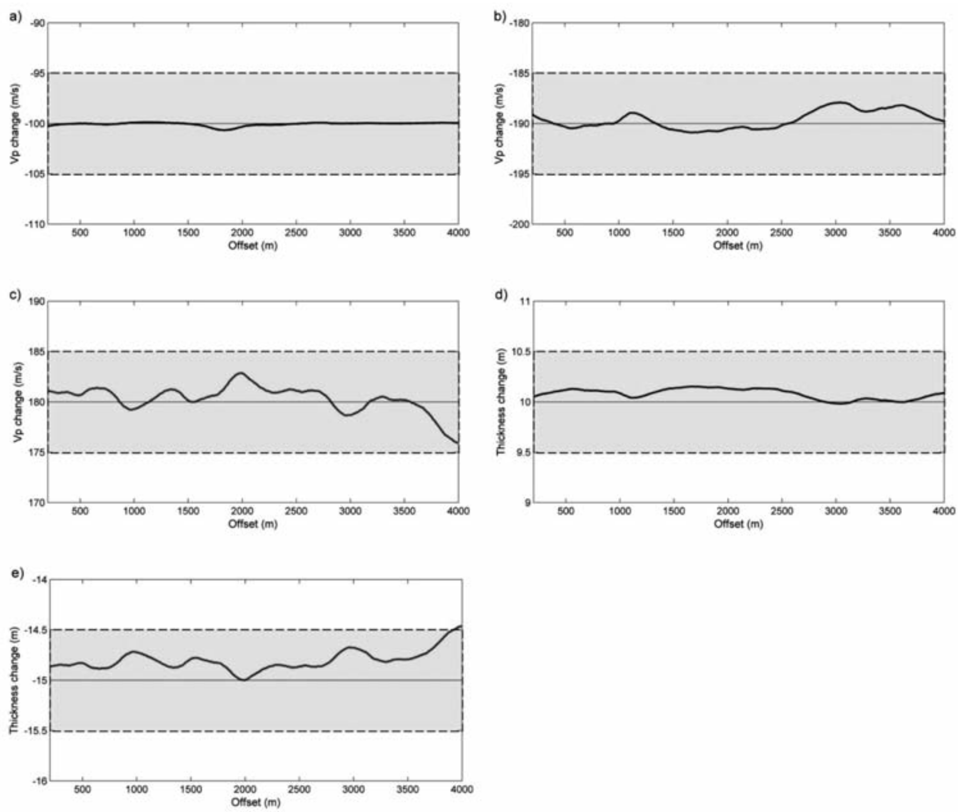

Fig. 3. The calculated changes in vertical velocity and layer thickness for interface one (a), interface two (b, d), and interface three (c, e) using vertical traveltime shift estimates and the 1D α-factor rock-physics model (calculated from the true earth model). In this figure, black thin curves represent the true reservoir model values and the thick curves represent the estimates based on the time-lapse τ-p algorithm. In (a), (b) and (c), the grey box indicates the error in velocity change estimates of ±5 m/s. In (d) and (e), the grey box indicates the error in thickness change estimates of ±0.5 m.

Generally, the 1D dilation-compaction R-factor or α-value is not known a priori and so represents another uncertainty in the time-lapse analysis. However, the method proposed by Røste et al. (2006) provides a process to estimate the dilation factor within a given layer. In Fig. 4, the two-way traveltime curves estimated utilizing the τ-p transform approach for the three interfaces for both the baseline and monitor models are displayed. Also shown is the difference between the calculated and the true earth model two-way traveltimes. Fig. 4(c) illustrates the differences between the predicted relative traveltime $\Delta T_0(x_0,d)/T_0(x_0,d)$ used to calculate the most optimal α-value for all offsets [eq. (17)] and that from the true reservoir model for both the top and bottom reservoir interfaces. Fig. 4(d) shows the estimated dilation factor (α) for the top and bottom reservoir horizons to yield the errors shown in Fig. 4(b).

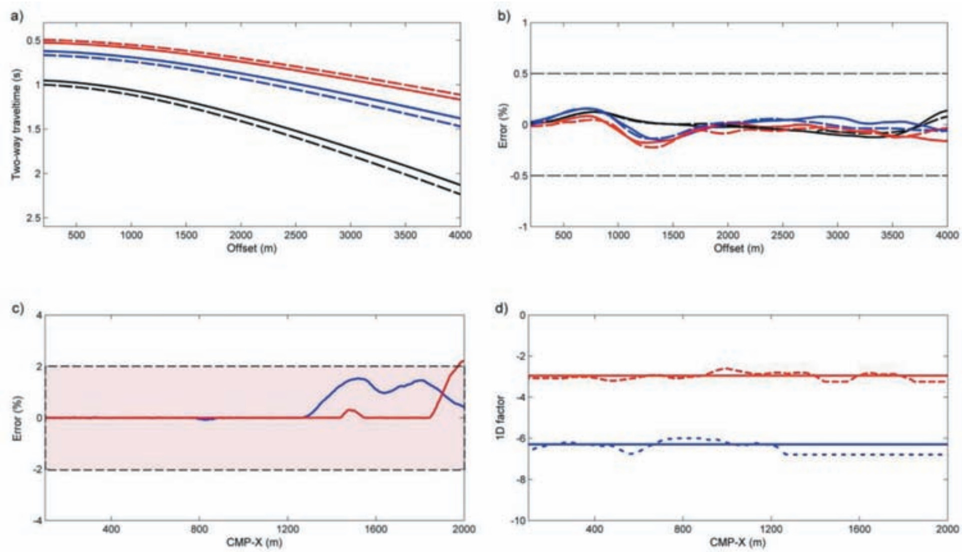

Fig. 4. Graphs (a) and (b) show the two-way traveltime estimates $T(x_0,d)$ and the errors calculated with respect to the true subsurface model, by applying the CMP gather τ-p transform approach for the three interfaces. Graph (c) shows the errors in relative traveltime shifts $\Delta T(x_0,d)/T(x_0,d)$ calculated from the differences between the predicted and the true reservoir model for the second and third interfaces. Graph (d) shows the τ-values estimates (dashed curves) and the true subsurface model values (solid curves) on interfaces two and three. In this figure, the black curve represents the values for interface one, blue curve for interface two, and red curve for interface three. In (a) and (b), the solid and dashed curves represent the estimates for baseline and monitor models, respectively.

Horizontal model with a dipping layer

In the presence of dipping reflectors and for the CMP geometry, the two-way traveltime equation for flat horizons [see eq. (1)] can be extended (Diebold and Stoffa, 1981)

$$t_{cmp} = \sum_i Z_i \cdot (q_{\uparrow i} + q_{\downarrow i}) + X(p_\uparrow + p_\downarrow) \quad , \qquad (18)$$

where X is half source-receiver offset, Z_i is the layer thickness, $p_\uparrow$ and $p_\downarrow$ are horizontal slowness for the up- and down-going rays, $q_{\uparrow i}$ and $q_{\downarrow i}$ are vertical slowness for the up- and down-going rays for individual layers (see Fig. 5a). For a flat model with horizontal layers, eq. (18) reduces to eq. (1).

We modify the previous four-layer elastic model and introduce a dipping layer for the top of the reservoir unit. The second horizon has a gentle dip of

3.6°, whereas the other interfaces remain horizontal. Fig. 5(b) and 5(c) display the CMP synthetic waveforms using both the ray tracing algorithm as well as the FD full-waveform algorithm. Figs. 5(d) and 5(e) show the associated transformation in the τ-p domain.

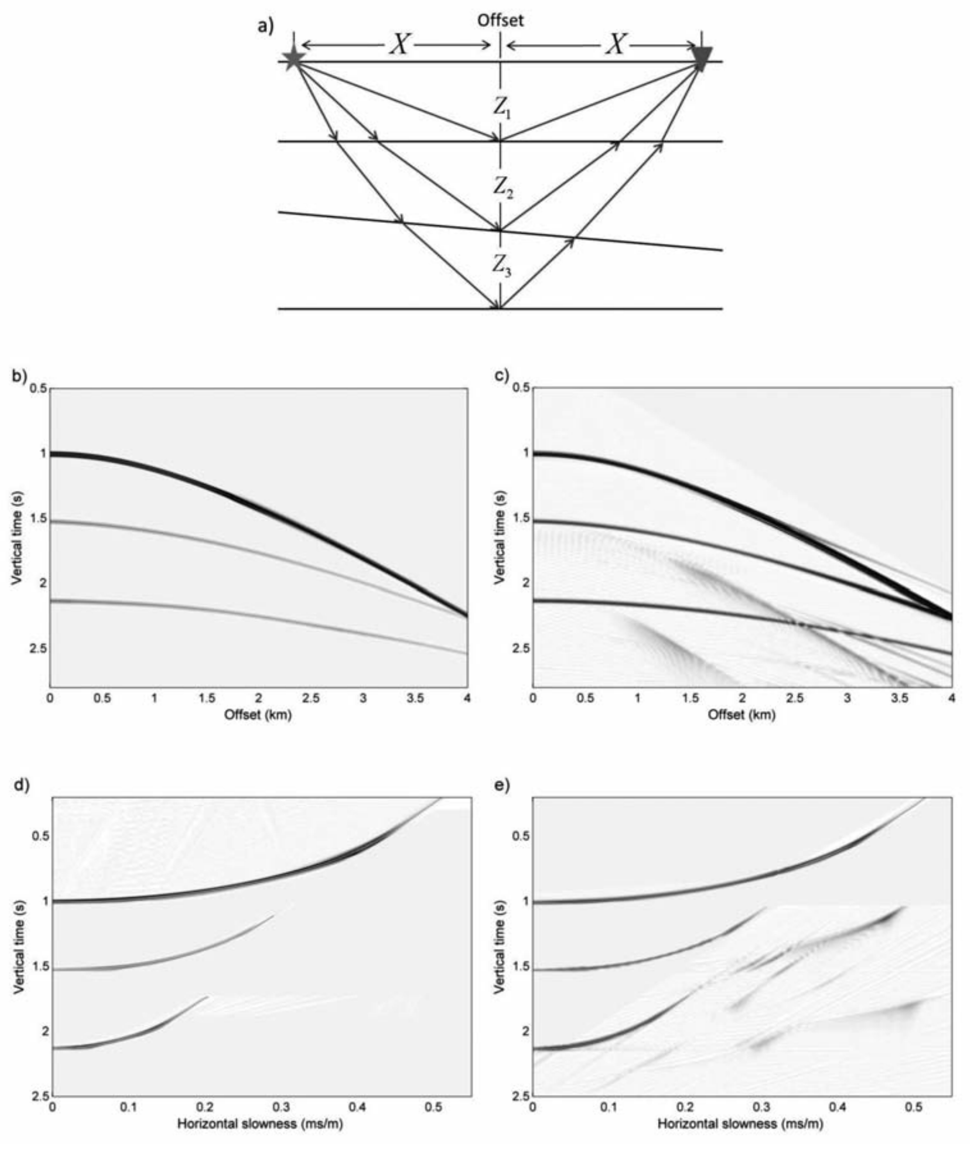

Fig. 5. Rays for the common-midpoint geometry of the dipping-layered model (a), the synthetic data for P-wave reflections from ray tracing (b) and finite-difference full-waveform modelling (c), and the associated mapping (d, e) in the τ-p domain.

The errors in vertical traveltime shifts calculated between the estimates for the ray tracing simulation and the true reservoir model values are displayed in Fig. 6(a), where midpoint is the reference. The differences are noticeable for the second (i.e., the dipping interface) and third horizons, but are still within tolerable range (± 1.5 ms, or $\pm 3.7\%$). This indicates dip has a minimal effect on performance of the method for calculating of interval vertical traveltime shifts for CMP geometry for layering homogeneous model, via using the averaged horizontal slowness of the up- and down-going rays. The predicted and true model α-values are shown in Fig. 6(b). For this particular dipping-layered model, the α-values estimates are comparable to those of the true subsurface model, with maximum error being 7.5%.

Fig. 6(c) displays the errors in vertical traveltime shifts computed between the FD synthetics and the true subsurface model for all three interfaces. The measured errors are within ± 1.5 ms, but are significantly noisier due to the presence of the interval multiples. In Fig. 6(d) the predicted and true α-values are shown, and indicate that multiples might have slight influence on the introduced time-lapse τ-p transform traveltime shifts and α-values calculation method.

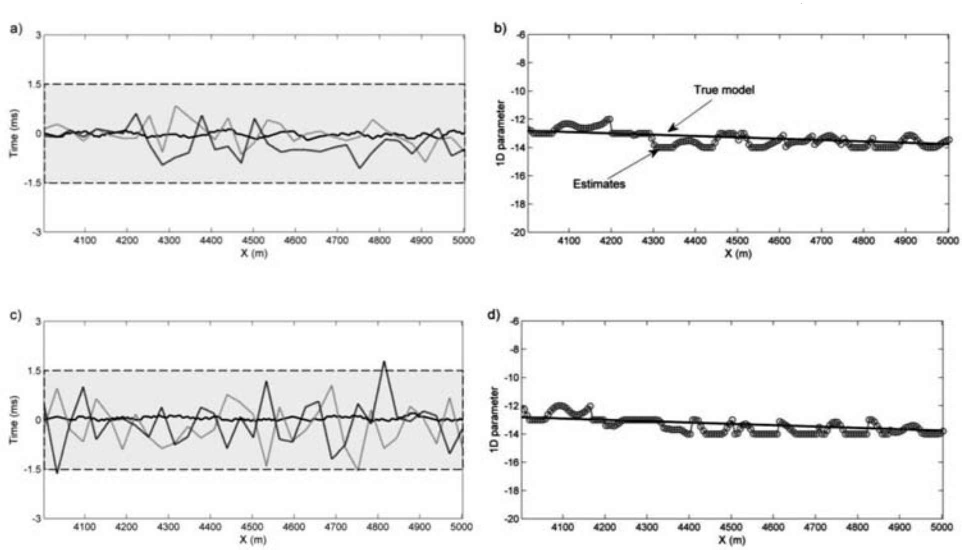

Fig. 6. Errors in the vertical travel-time shifts estimates calculated from the differences compared with the true subsurface model values for three horizons (a, c) and the estimated a-values displayed with the true earth model values for the dipping layer (b, d), for the ray tracing and finite-difference methods respectively. In graphs (a) and (c), the black solid curve represents the horizon one, the grey dotted curve represents horizon two and the black dotted curve represents horizon three. In graphs (b) and (d), the grey circles represent the estimated τ-value and the black curve represents the true earth model value. The grey box in (a) and (c) indicates the maximum tolerable error of ± 1.5 ms.

Velocity anisotropy effects

We consider the horizontal four-layer reservoir model, but introduce VTI anisotropy within the overburden unit above the reservoir. The other layers are kept isotropic. In this model, we want to evaluate the influence of induced seismic anisotropy on the layer interval vertical traveltime shifts estimates using the pre-stack gather τ-p transform method. Time-lapse seismic synthetics for P-P wave reflections are generated using the anisotropic ray tracer ATRAK. In our analysis, two ranges of Thomsen anisotropic parameters (Thomsen, 1986) are used, where both time-lapse static (natural) and induced seismic anisotropy are examined (e.g., six cases). In the first case, the medium is weakly VTI with parameters $\varepsilon = 0.255$, $\delta = -0.050$, and $\eta = 0.339$. Whereas in the second case the medium is strongly VTI with parameters $\varepsilon = 0.334$, $\delta = 0.730$, and $\eta = -0.161$.

For the first case shown in Fig. 7(a), both baseline and monitor models are isotropic and represents the case where no velocity anisotropy develops, and only isotropic velocity changes and strains develop (e.g., Fig. 2a). In the second case (Fig. 7b), the medium is weakly seismically anisotropic for both the baseline and monitor models, but where isotropic changes and strains develop due to production to investigate the influence of static (i.e., non-production related) anisotropy on vertical time-shifts estimates. In the third case (Fig. 7c) the reservoir is initially isotropic where hydrocarbon production leads to stress-induced weak seismic anisotropy in the overburden. For the fourth case (Fig. 7d), we assume that both baseline and monitor models have an initial static strong seismic anisotropy, but where isotropic velocity changes develop as well as strain. In the fifth case (Fig. 7e) the baseline model is isotropic, where significant time-lapse subsurface changes lead also to strong seismic anisotropy. Finally, the sixth model (Fig. 7f) consists of a weakly anisotropic baseline model, where production induces strong anisotropy in the monitor model. The corresponding errors in vertical traveltime shifts for three interfaces (i.e., overburden, top and bottom reservoir) are calculated and compared with the true subsurface model values. In all cases, the deviations are within ± 1.5 ms for all offsets, with the exception of the induced strong anisotropic cases five and six. This indicates that time-lapse induced seismic anisotropy can produce slight impact on the measured vertical traveltime shifts using the τ-p transform pre-stack method, whereas the time-lapse isotropic velocity changes in the presence of background anisotropy generate negligible effects. Therefore, the influence of background anisotropy and/or induced anisotropy does not strongly affect the estimating of layer interval vertical traveltime shifts using the seismic pre-stack gather τ-p transform method. It should be noted that the time-lapse seismic anisotropy in layer two has negligible influence on the estimated vertical traveltime shifts for layer three (i.e., red curve) when compared with the measurements for the medium anisotropy layer. This suggests that the overburden anisotropy has insignificant impact on the vertical traveltime shift estimates for the deeper layer. And thus it indicates the superiority of the introduced time-lapse seismic pre-stack τ-p transform vertical traveltime shifts calculations method over the conventional methods, in which the induced overburden velocity anisotropy and heterogeneity might impose significant impact on the deeper layers and hence could lead to errors in subsequent time-lapse seismic attributes estimations.

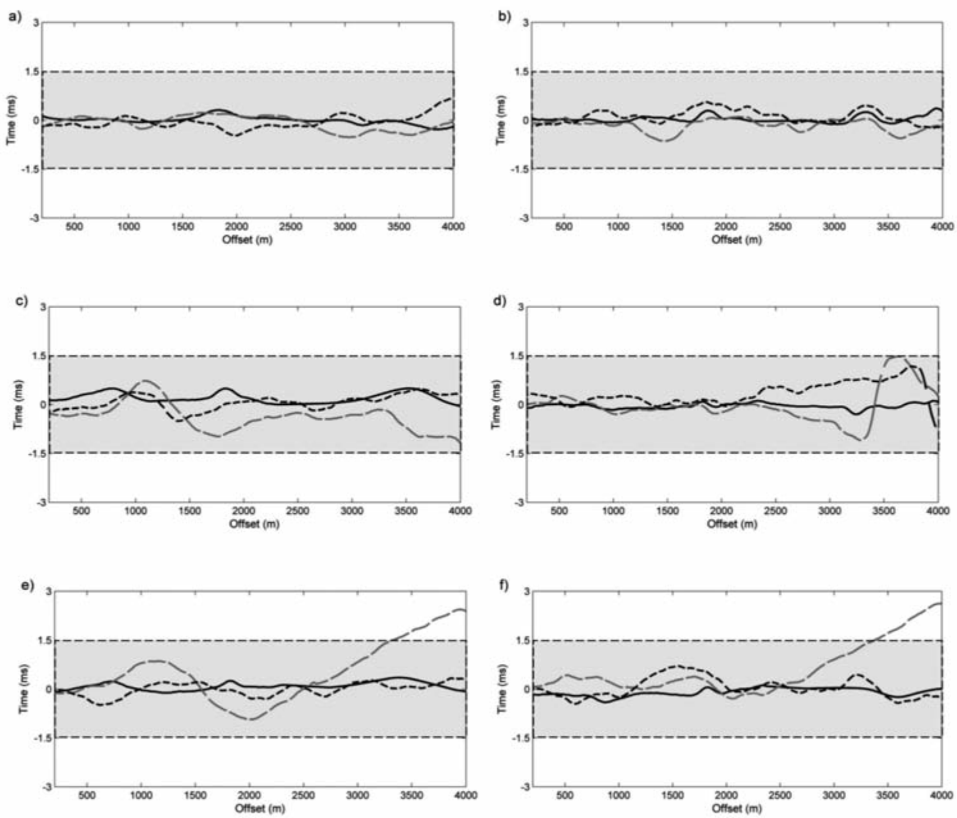

Fig. 7. The errors in time-lapse seismic vertical traveltime shifts estimates calculated from the differences with respect to the true reservoir model for three interfaces: (a) both baseline and monitor models are isotropic (i.e., Fig. 2a), (b) both baseline and monitor models have the same velocity anisotropy (weak VTI) in the second layer (case two), (c) baseline is isotropic and weak velocity anisotropy is induced in the monitor model (case three), (d) both baseline and monitor models have the same (strong) velocity anisotropy (case four), (e) baseline is isotropic and strong velocity anisotropy is induced in the monitor model (case five), and (f) baseline is weakly anisotropic and strong velocity anisotropy is induced in the monitor model (case six). The black solid curve represents interface one, the grey long dashed curve represents interface two, and the black short dashed curve represents interface three. The grey box indicates the maximum tolerable error of ± 1.5ms.

Deep reservoir model undergoing depletion

In the final experiment, a more realistic reservoir model is applied to examine the applicability of the pre-stack τ-p transform method for calculating layer-interval vertical traveltime shift for conditions of non-planar surfaces and velocity heterogeneity. The synthetic dynamic elastic model (He et al., 2015b,

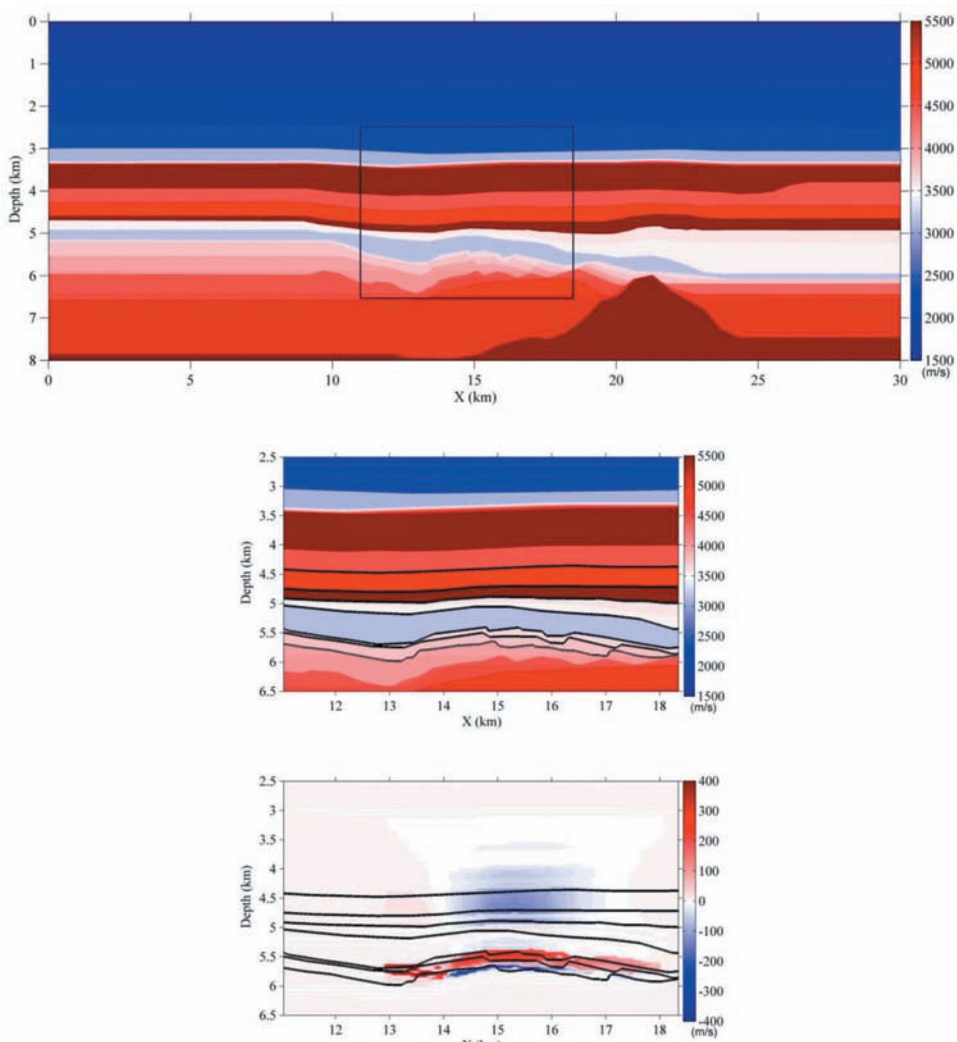

Fig. 8. The top figure is the P-wave velocity model for the hydro-mechanical deep reservoir model. The middle figure is a zoom in of the area of interest within the model showing the layer interfaces. The bottom figure shows the P-wave velocity change between the baseline and monitor surveys, where it can be seen that strong vertical and lateral velocity changes are induced as well as the complex layer geometries. In the middle and bottom figures, the black curves represent (from top to bottom) interfaces 7, 8, 9, 10, 11, 12 and 13, respectively.

in review) is built from a hydro-geomechanical model based on the structure and rock properties of deep reservoir undergoing depletion (Fig. 8). A non-linear rock physics relationship (Shapiro, 2003) is utilized to convert the effective stress changes into velocity changes within the reservoir and non-reservoir rocks. Significant velocity decreases in the overburden and velocity increases in the reservoir. In layers 8 and 9 (i.e., overburden) rock expansion leads to positive traveltime shifts, whereas in layer 12 (i.e., reservoir) compaction leads to negative traveltime shifts (see Fig. 8). Time-lapse synthetic seismograms are generated by using the isotropic FD algorithm E3D to simulate more realistic seismic responses. The shots are located between 10631 m and 17831 m with shot interval of 50 m. A total of 360 receivers are used for each shot, with receiver interval of 12.5 m. Only positive offset data are used with the smallest shot-receiver offset being 175 m and the largest shot-receiver offset being 4662.5 m.

In Fig. 9, the vertical traveltime shifts estimated from post-stack migrated data of near-offset gathers and cross-correlation algorithm (He et al., 2015b) are compared with the estimates of the time-lapse τ-p transform method. It can be seen that the time-lapse τ-p transform method provides improved estimates of layer-interval vertical traveltime shifts for layers 8, 9 and 12 compared to those of the cross-correlation algorithm. This is because the post-stack cross-correlation method might be biased by complex underground geometry, time-lapse noise, migration method and time-window size (e.g., Cox and Hatchell, 2008; Selwood, 2010). Although the estimates in the overburden are slightly better than those in the reservoir, the τ-p PSITS method still produces reasonably accurate time-lapse traveltime shifts estimates in the deep reservoir compartment (layer 12) even with the presence of complex geometry and strong induced velocity heterogeneity. The errors calculated with respect to the true model values are less than ± 1.5 ms for the most reservoir layer.

DISCUSSION

The results of the four-layer and the deep reservoir models undergoing depletion show that the τ-p PSITS approach is straightforward to implement. Furthermore, it has the advantage over conventional cross-correlation traveltime shift estimation algorithms that require suitable time-window sizes and post-stack data because it reduces the amount of processing and hence processing errors (e.g., migration velocity model building). More importantly, the τ-p PSITS approach establishes a practical capability for obtaining robust estimates of time-lapse traveltime shifts as well as the 1D velocity-strain parameter. The proposed time-lapse seismic interpretation method, which does not require any amplitude analysis and thus avoids other possible sources of errors, has the potential to yield more accurate traveltime shifts to discriminate between changes in vertical velocity and strain for individual layers and that is free from the overburden effects. By means of the layer stripping algorithm, time-lapse attributes are calculated in a layer-by-layer fashion.

Due to the high repeatability and quality for the time-lapse seismic synthetic data, no specific pre-processing was needed to enhance signal quality. However, in the presence of signal noise and acquisition repeatability issues, artefacts would likely be present in the τ-p transform (e.g., Kappus et al., 1990). For field data with low signal-to-noise ratio and strong layer interval multiples, time-windows can be applied for specific offset ranges to isolate traveltime events. Various source wavelets and uncertainties in acquisition geometry repeatability will likely introduce errors in the τ-p PSITS approach.

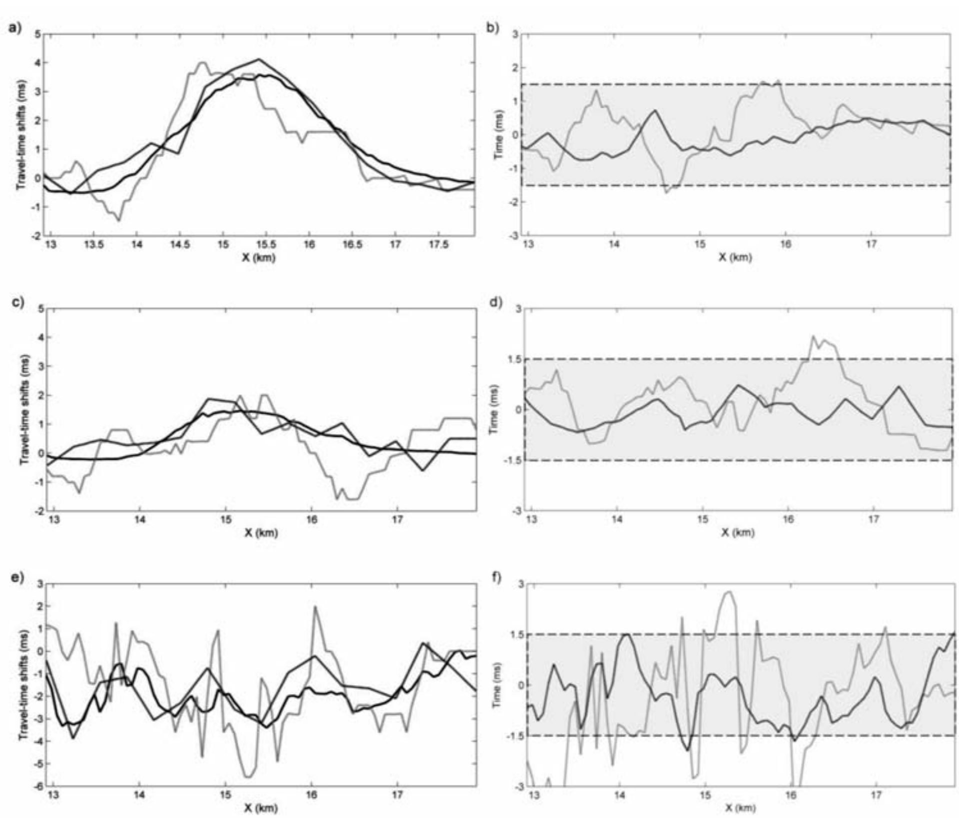

Fig. 9. The left column shows the time-lapse seismic vertical traveltime shifts for (top) layer 8 (between interfaces 7 and 8), (middle) layer 9 (between interfaces 8 and 9) and (bottom) layer 12 (between interfaces 11 and 12), respectively. The right column shows the errors in vertical traveltime shifts estimates for layers 8, 9 and 12, respectively. In this figure, the black solid curve represents the true model value, the grey dotted curve represents the estimates using the cross-correlation algorithm and post-stack migrated data (He et al., 2015b), and the black dotted curve represents the estimates using the τ-p PSITS method. The grey box represents the maximum tolerable error of ± 1.5 ms.

These influences could be significant, and hence further research is needed to develop pre-processing sequences as well as understand their impact on time-lapse real data attributes analysis.

The influence of time-lapse seismic anisotropy on layer interval traveltime shifts estimates was examined using the pre-stack τ-p transform method. We focus on VTI seismic anisotropy as well as P-P wave reflections only. The method, however, should be applicable to other wave modes, such as P-S mode converted waves, as well as models having horizontal transverse isotropy.

The subsurface time-lapse seismic traveltime shift is possibly affected by changes in ray path as well as velocity. Typically, the contribution of strain component to the total traveltime shift is much smaller than that of velocity changes. Although we assume a 1D strain-velocity model, both strain and seismic velocities are dependent on the evolution of the triaxial stress state (see Herwanger, 2011). Thus the 1D rock physics model may not be appropriate in complex geometries influenced by stress-arching and compartmentalisation. Therefore, it is important to note that horizontal stress and strain changes could introduce significant distortion in traveltime shifts, and thus need to be taken into consideration when predicting the time-lapse vertical velocity and strain changes. In that case, 3D numerical geomechanical modelling can be used, in conjunction with laboratory core data and well logging measurements, to refine the relationships for velocity-stress and velocity-strain data.

CONCLUSIONS

Reservoir fluid extraction and re-injection can lead to significant subsurface time-lapse changes, for instance velocity change and strain, on time-lapse seismic data within a reservoir and the surrounding rocks. In this paper, time-lapse seismic vertical traveltime shifts are estimated directly for individual layers utilizing the seismic pre-stack data (shot and CMP gathers) and τ-p transform method, and the estimates are compared with the measurements using cross-correlation method and post-stack migrated data. The changes in vertical velocity and layer thickness are calculated using the estimated vertical traveltime shifts and the 1D α-factor velocity-strain relationship. The method has been applied to not only the four-layer reservoir models, but also on a complex deep reservoir model undergoing depletion. The results for the P-P wave subcritical reflections, using both ray tracing and FD full-waveform methods, for horizontal and gently dipping layers, induced isotropic and anisotropic velocity changes, and non-planar surface and strong lateral velocity heterogeneity indicate that time-lapse seismic pre-stack gather using the τ-p transform method has strong potential to yield highly accurate layer-interval vertical traveltime shifts estimates and hence to help discriminate between reservoir compaction and vertical velocity changes.

ACKNOWLEDGEMENTS

Yanxiao He would like to thank the China Scholarship Council and University of Leeds for the financial support. We are grateful to the Seismic Geomechanics Group, University of Leeds for supporting this study. We acknowledge Total E&P UK Ltd. for providing the complex deep reservoir model. We also thank Rockfield Software for access to the geomechanical model builder RMS(TEMPEST).

REFERENCES

Alkhalifah, T., 1998. Acoustic approximations for processing in transversely isotropic media. Geophysics, 63: 623-631.

Alkhalifah, T. and Tsvankin, I. 1995. Velocity analysis for transversely isotropic media. Geophysics, 60: 1550-1566.

Angus, D.A., Verdon, J.P., Fisher, Q.J., Kendall, J.-M., Segura, J.M., Kristiansen, T.G., Crook, A.J.L., Skachkov, S., Yu, J. and Dutko, M., 2011. Integrated fluid-flow, geomechanic and seismic modelling for reservoir characterization. Recorder, Can. SEG, 36: 27-36.

Chapman, C.H., 1981. Generalized Randon transforms and slant stacks. Geophys. J. Roy. Astronom. Soc., 66: 445-453.

Cox, B. and Hatchell, P., 2008. Straightening out lateral shifts in time-lapse seismic. First Break, 26: 93-98.

Diebold, J.B. and Stoffa, P.L., 1981. The traveltime equation, tau-p mapping, and inversion of common midpoint data. Geophysics, 46: 238-254.

Fuck, R.F., Bakulin, A. and Tsvankin, I., 2009. Theory of traveltime shifts around compacting reservoir: 3D solution for heterogeneous anisotropic media. Geophysics, 74: D25-D36.

Ghaderi, A. and Landrø, M., 2009. Estimation of thickness and velocity changes of injected carbon dioxide layers from prestack time-lapse seismic data. Geophysics, 74(2): O17-O28.

Guest, W.S. and Kendall, J.-M., 1993. Modelling seismic waveforms in anisotropic inhomogeneous media using ray and Maslov asymptotic theory: Applications to exploration seismology. Can. J. Expl. Geophys., 29: 78-92.

Hatchell, P. and Bourne, S., 2005. Rocks under strain: Strain-induced time-lapse time-shifts are observed for depleting reservoirs. The Leading Edge, 12: 1222-1225.

He, Y.-X. and Angus, D.A., 2014. Pre-stack time-lapse seismic attributes analysis in tau-p domain. Extended Abstr., 76th EAGE Conf., Amsterdam: We-P06-01.

He, Y.-X., Angus, D.A., Clark, R.A. and Hildyard, M.W., 2015(a). Analysis of time-lapse travel-time and amplitude changes to assess reservoir compartmentalization. Geophys. Prosp., doi: 10.1111/1365-2478.12250.

He, Y.-X., Angus, D.A., Blanchard, T.D., Wang, G.-L., Yuan, S.-Y., and Garcia, A., 2015(b). Time-lapse seismic waveform modelling and analysis using hydro-mechanical models for a deep reservoir undergoing depletion. Submitted to Geophys. J. Internat.

Herwanger, J.V. and Koutsabeloulis, N., 2011. Seismic Geomechanics: How to Build and Calibrate Geomechanical Models using 3D and 4D Seismic Data. EAGE, Houten.

Kappus, M.E., Harding, A.J. and Orcutt, J.A., 1990. A comparison of tau-p transform methods. Geophysics, 55: 1202-1215.

Landrø, M. and Stammeijer, J., 2004. Quantitative estimation of compaction and velocity changes using 4D impedance and traveltime changes. Geophysics, 69: 949-957.

Larsen, S., Wiley, R., Roberts, P. and House, L., 2001. Next-generation numerical modelling: incorporating elasticity, anisotropy and attenuation. Expanded Abstr., 71st Ann. Internat. SEG Mtg., San Antonio: 1218-1221.

Reine, C., Clark, R. and van der Baan, M., 2012. Robust prestack Q-determination using surface seismic data: Part 1 - Method and synthetic examples. Geophysics, 77: R45-R56.

Røste, T., Stovas, A. and Landrø, M., 2005. Estimation of layer thickness and velocity change using 4D prestack seismic data. Extended Abstr., 67th EAGE Conf., Madrid: C010.

Røste, T., Stovas, A. and Landrø, M., 2006. Estimation of layer thickness and velocity changes using 4D prestack seismic data. Geophysics, 71(6): S219-S234.

Selwood, C., 2010. Researching the Optimum Bandwidth to Extract 4D Time Shifts. M.Sc. Thesis, University of Leeds, Leeds.

Shapiro, S.A., 2003. Elastic piezosensitivity of porous and fractured rocks. Geophysics, 68: 1954-1966.

Smith, S.S. and Tsvankin, I., 2012. Modelling and analysis of compaction-induced traveltime shifts for multicomponent seismic data. Geophysics, 77(6): T221-T237.

Stoffa, P.L., Buhl, P., Diebold, J. and Wenzel, F., 1981. Direct mapping of seismic data to the domain of intercept time and ray parameter - A plane wave decomposition. Geophysics, 46: 255-267.

Thomsen, L., 1986. Weak elastic anisotropy. Geophysics, 51: 1954-1966.

van der Baan, M. and Kendall, J.-M., 2002. Estimating anisotropy parameters and traveltimes in the tau-p domain. Geophysics, 67:1076-1086.

van der Baan, M. and Kendall, J.-M., 2003. Traveltime and conversion-point computations and parameter estimation in layered, anisotropic media by τ-p transform. Geophysics, 68: 210-224.